Received: 30 March 2021 | Revised: 25 July 2021 | Accepted: 26 July 2021

DOI: 10.1002/jrs.6228

SPECIAL ISSUE - RESEARCH ARTICLE

Journal of RAMAN SPECTROSCOPY WILEY

Interference-enhanced deep-ultraviolet Raman signals of hexagonal boron nitride flake and its underlying silicon substrate

Tao Liu[1,2] | Miao-Ling Lin[1] | Yu-Chen Leng[1,2] | Xin Cong[1,2] | Xin Zhang[1] | Ping-Heng Tan[1,2]

[1]State Key Laboratory of Superlattices and Microstructures, Institute of Semiconductors, Chinese Academy of Sciences, Beijing, 100083, China

[2]Center of Materials Science and Optoelectronics Engineering & CAS Center of Excellence in Topological Quantum Computation, University of Chinese Academy of Sciences, Beijing, 100049, China

Correspondence
Ping-Heng Tan, State Key Laboratory of Superlattices and Microstructures, Institute of Semiconductors, Chinese Academy of Sciences, Beijing 100083, China.
Email: phtan@semi.ac.cn

Funding information
National Key Research and Development Program of China, Grant/Award Number: 2016YFA0301204; National Natural Science Foundation of China, Grant/Award Numbers: 11874350, 12004377

Abstract

We take hexagonal boron nitride (hBN) flakes exfoliated on SiO_2/Si substrates as a prototype, to demonstrate how to enhance the Raman signals both from ultra-thin layered materials and the underlying opaque substrate excited by deep ultraviolet (DUV) laser. We found that the interference effect in the hBN/SiO_2/Si multilayered structure can largely enhance Raman intensity of hBN flake and the underlying Si substrate under 266-nm excitation. This enhancement effect is more significant than that under visible excitation. With increasing the thickness of SiO_2 layer in the substrate, the corresponding hBN and Si Raman intensity can vary by up to ~ 4 and ~2 orders of magnitude under 266-nm excitation, respectively. This method can be applicable to enhance Raman signal from other two-dimensional materials under DUV excitation by tuning the thickness of SiO_2 layer in the SiO_2/Si substrate.

KEYWORDS

deep ultraviolet excitation, hexagonal boron nitride, interference effect, multilayered dielectric structure, two-dimensional material

1 | INTRODUCTION

As a fingerprint of materials of interest, Raman spectroscopy has been widely used to characterize the crystal structure, electronic band structure and phonon dispersion of crystals.[1-3] The Raman intensity under non-resonant condition is proportional to the fourth power of excitation energy. Therefore, deep ultraviolet (DUV) lasers are widely used to enhance Raman intensity of materials. However, the penetration depth of DUV lasers in opaque materials is usually very small, which can reach down to a nanometer scale. This results in that the DUV Raman signal of opaque materials may be very weak because of the small effective sample volume contributed to Raman scattering. In addition, the photon energy of DUV lasers is quite large, resulting in heating or damage of opaque materials with low thermal conductivity. Furthermore, under DUV excitation, the thermally activated chemical reactions facilitate the formation of a carbonaceous contamination layer on the surface of sample, which reduces the Raman intensity of the material of interest, including transparent films on substrates.[4] Therefore, the power of DUV laser is usually limited and much lower than that of visible or near infrared laser. These factors make it uneasy to study DUV Raman spectroscopy of ultrathin flakes of opaque materials and transparent films, such as two-dimensional materials (2DMs) and related heterostructures.[5,6]

Ultrathin 2DM flakes, e.g., hexagonal boron nitride (hBN) flakes, are usually deposited or exfoliated on a dielectric substrate, such as SiO_2/Si substrate (i.e., Si substrate covered by a SiO_2 film). The 2DM flake and its underlying SiO_2/Si substrate will form a multilayered dielectric structure. When a laser beam is incident to the surface of 2DM flake on SiO_2/Si substrate, it undergoes multiple reflections and refractions at the interfaces in the multilayered structure, giving rise to an interference effect.[7-10] This effect makes optical contrast of 2DM flakes dependent on the thickness of SiO_2 layer (d_{SiO_2}) and the number of layers (N) of 2DM flakes, which is used to quickly identify N of 2DM flakes on SiO_2/Si substrate.[11,12] This interference effect will also modulate the intensity of laser and Raman signal within the multilayered structure. A number of studies demonstrated that this effect can enhance or reduce the Raman signal of the 2DM flake on SiO_2/Si substrate in visible region.[8–10,13,14] However, the modulations of the DUV Raman intensity from the ultrathin 2DM flake on multilayered substrate remain unexplored. It is still an open question whether it is possible to enhance the DUV Raman signal of the material of interest by constructing a suitable multilayered structure.

In this work, we constructed a hBN/SiO_2/Si multilayered structure by exfoliating NL-hBN flakes onto SiO_2/Si substrate. Under 266-nm excitation, Raman intensities of Si and hBN first increase and then decrease as N increases. This arises from the interference effect in hBN/SiO_2/Si multilayered structure, which is confirmed by the calculation based on transfer matrix formalism. Raman intensities of hBN and Si as functions of d_{SiO_2} and N are also calculated to obtain full pictures of the interference-enhanced effect on Raman intensity of hBN and Si in hBN/SiO_2/Si multilayered structure, where d_{SiO_2} varies from 0 to 500 nm, and N varies from 0 to 1000. Upon choosing an optimum of d_{SiO_2} for a given hBN thickness, the Raman intensity of hBN can be greatly enhanced under the 266-nm excitation.

2 | EXPERIMENTAL

The NL-hBN flakes were mechanically exfoliated from bulk hBN onto 90-nm SiO_2/Si substrates. The thickness of SiO_2 layer was determined by a spectroscopic ellipsometer.[10] The atomic force microscopy (AFM) was used to measure the thickness of NL-hBN flakes and the corresponding N with a tapping mode. Raman measurements of hBN flakes and the underlying Si substrate were performed in backscattering geometry at room temperature using Jobin-Yvon HR800 and T64000 micro-Raman systems. Each system is equipped with a 2400 lines mm^{-1} grating and a charge-coupled detectors (CCD) cooled by liquid nitrogen.

The HR800 micro-Raman system is equipped with a $\times$100 objective lens with a NA of $\sim$0.9 and the excitation wavelength is 532 nm from a diode-pumped solid-state laser. The T64000 micro-Raman system is equipped with a $\times$74 objective lens with a NA of $\sim$0.66 and the excitation wavelength is 266 nm from a diode-pumped solid-state laser. The laser power was less than 1 mW for 532 nm and 140 μW for 266 nm to avoid sample heating. The resolutions of the Raman system are 1.06 cm^{-1} and 0.31 cm^{-1} per CCD pixel at 266 nm and 532 nm, respectively. For the Raman measurement of each flake, we focused the laser on the bare substrate close to the edge of hBN flake to get a maximum Raman intensity of Si by adjusting the focus of the microscope, then moved the motorized stage to make the laser spot on the hBN flake without changing the focus of the microscope and measured Raman signal from the hBN flake and the underlying Si substrate.

3 | RESULTS AND DISCUSSIONS

Figures 1(a) and (b) show the Raman spectra from a bulk Si and a thick hBN flake with a thickness of more than 10 μm excited by 532 nm and 266 nm lasers, respectively. All Raman peaks of the thick hBN flake are normalized by the intensity of Si peak under the same experimental condition. The Raman signal of bulk Si is stronger than that of the thick hBN flake excited by 532-nm laser, while the Si Raman signal is much weaker than the hBN Raman signal under the 266-nm excitation. This difference mainly results from the significant difference between penetration depths of 266-nm laser in Si and hBN. hBN is a wide-bandgap semiconductor material with a bandgap of $\sim$ 5.9 eV ($\sim$ 210 nm), leading to its weak absorption and large penetration depth of lasers at both 532 nm and 266 nm. However, the absorption coefficient of Si is remarkably large in the UV region, and the penetration depth of 266-nm laser in Si is only $\sim$5 nm.[15] This makes its Raman signal excited by 266 nm laser much smaller than that of the thick hBN flake.

We prepared NL-hBN flakes on SiO_2/Si substrates by mechanical exfoliation. A typical optical image of a hBN flake is shown in Figure 2(a). The AFM image of the hBN flake is shown in the inset of Figure 2(a), and its measured thickness (22.3 nm) corresponds to 67L. Figure 2(b) shows the schematic diagrams for light propagation of laser and Raman signals from Si, where I_{bulk}(Si) and I_{2-NL}(Si) are the Raman intensities (i.e., peak height) of Si from bulk Si and SiO_2/Si substrate underneath an NL-hBN flake. Figures 2(c) and (d) depict

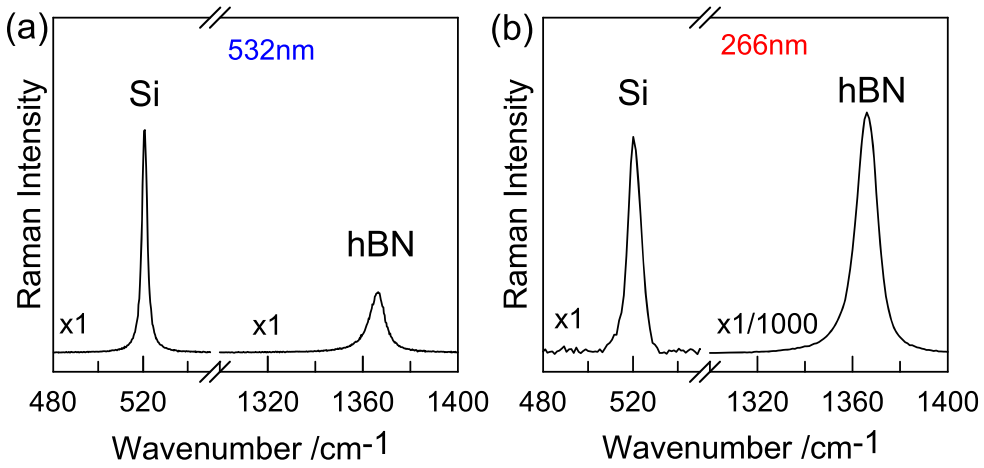

FIGURE 1 Raman spectra of bulk Si and thick hBN flake with a thickness of more than 10 μm excited by (a) 532-nm and (b) 266-nm lasers

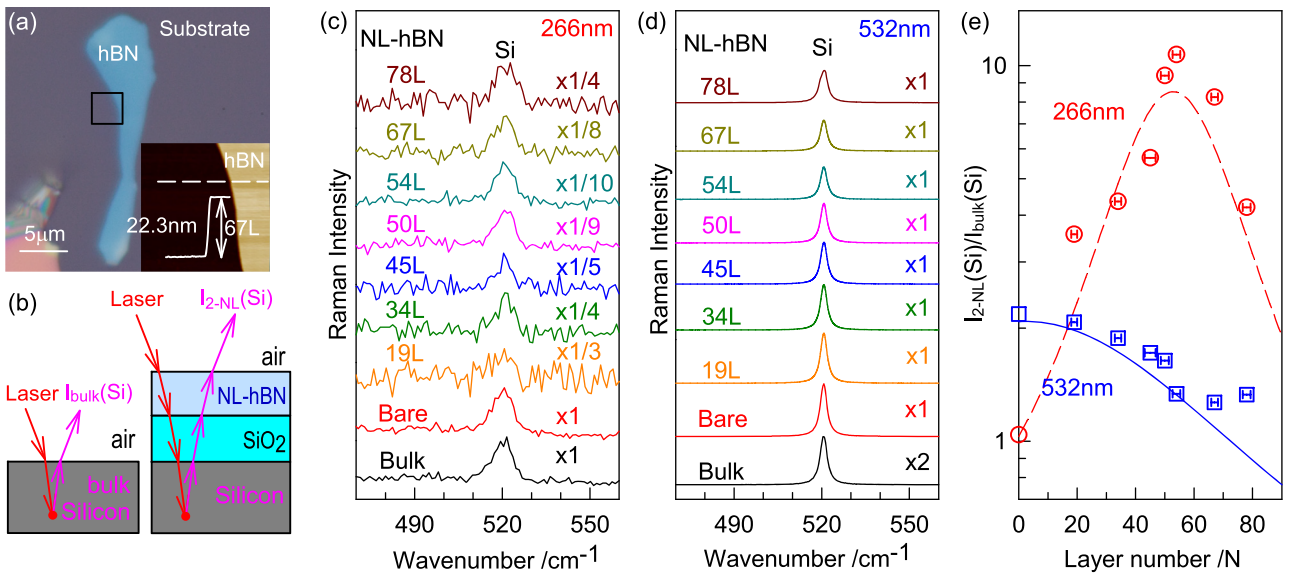

FIGURE 2 (a) Optical image of 67L-hBN flake on a 90-nm SiO_2/Si substrate. The inset shows AFM image of the sample along with the height profile along the dash line. (b) Schematic diagrams for light propagation of laser and Si Raman signals from bulk Si and *N*L-hBN/SiO_2/Si structure. Raman spectra from bulk Si and SiO_2/Si substrate underneath *N*L-hBN flakes under (c) 266-nm and (d) 532-nm excitations, respectively. (e) $I_{2-NL}(Si)/I_{bulk}(Si)$ as a function of *N* when d_{SiO_2}=90 nm. Circles and squares indicate the experimental data while the dash and solid lines are the calculated results

Raman spectra of bulk Si and Si substrates underneath *N*L-hBN flakes under 266-nm and 532-nm excitations, respectively, where "Bare" indicates *N*=0, i.e., SiO_2/Si substrate without any coverage of hBN flakes. All Raman spectra are normalized by $I_{bulk}(Si)$. Under 266-nm excitation, $I_{2-NL}(Si)$ first increases and then decreases with increasing *N*, reaching a maximum at 54L. However, $I_{2-NL}(Si)$ decreases monotonically with *N* under 532-nm excitation. The measured $I_{2-NL}(Si)/I_{bulk}(Si)$ as a function of *N* are summarized in Figure 2(e) for both 532-nm and 266-nm excitations.

N-dependent $I_{2-NL}(Si)/I_{bulk}(Si)$ can be explained by the interference effect arising from multiple reflections and refractions of laser and Raman signal in a hBN/SiO_2/Si multilayered structure. This interference effect may increase or reduce the intensity of laser beam and Raman signals in the multilayered structure.[10] According to the Raman results excited by visible lasers, $I_{2-NL}(Si)$ depends on *N*, excitation wavelength and the NA of the objective.[8–10,13,14]Nevertheless, in this work, we focused on the normalized Raman intensity(e.g. $I_{2-NL}(Si)/I_{bulk}(Si)$), and thus, the influence from NA can be nearly cancelled out, which has been discussed in the previous work.[10] For simplicity, we assume normal incidence in this work, i.e., the NA of microscope objective is assumed as 0. In this case, the

intensity of Raman signal from the medium i in the multilayered structure can be expressed by the following equation[10]:

$$I \propto \int_0^{d_i} |F_L(z_i) \cdot F_R(z_i)|^2 dz_i, \quad (1)$$

where z_i is the depth of Raman scattering source in the medium i, and d_i is the thickness of the medium i. F_L and F_R are enhancement factors, indicating the influence of interference effect on the laser beam and Raman signal in the multilayered structure, respectively. The enhancement factors can be calculated by transfer matrix formalism, which has been widely used to calculate the Raman intensity and optical contrast of 2D flakes on SiO_2/Si substrates.[10,12–14,16] The complex refractive indices of Si and hBN are functions of wavelengths of laser beam (λ_L) and Raman signal (λ_R)[15,17,18] and the difference between λ_L and λ_R must be considered during the calculation.[9] I_{2-NL}(Si) can be obtained by substituting F_L and F_R into equation (1). I_{bulk}(Si) can be also calculated by setting d_{hBN} and d_{SiO_2} to 0. The dash and solid lines in Figure 2(e), respectively, show the calculated N -dependent I_{2-NL}(Si)/I_{bulk}(Si) under 266-nm and 532-nm excitations. It clearly suggests that the interference effect in the multilayered structure has completely different influences on Raman intensity excited by DUV and visible excitations.

The interference effect of laser and Raman signal in the NL-hBN/SiO_2/Si multilayered structure is related to N, as shown in Figure 2(e). This effect is also dependent on d_{SiO_2}, which may enhance the Raman signal from SiO_2/Si substrate. Figure 3(a) shows the I_{2-NL}(Si)/I_{bulk}(Si) calculated by transfer matrix formalism as a function of N and d_{SiO_2} under 266-nm excitation. By adjusting N and d_{SiO_2}, relative to the Raman intensity of bulk Si, the intensity of Si Raman signal from the multilayered structure can be reduced or increased up to ~10 times. Indeed, the experimental I_{2-NL}(Si)/I_{bulk}(Si) in Figure 2 (e) has been enhanced about 10 times when $N = 54$. The curves of I_{2-NL}(Si)/I_{bulk}(Si) for $N = 1$ and $N = 66$ from SiO_2/Si substrate with different thickness of SiO_2 layer are given in Figure 3(b). For $N = 1$, I_{2-NL}(Si)/I_{bulk}(Si) varies in a small range from ~0.9 to ~2.8, while I_{2-NL}(Si)/I_{bulk}(Si) varies by nearly 2 orders of magnitude for $N = 66$. Therefore, for a given N, an appropriate d_{SiO_2} is a critical factor to enhance DUV Raman signal of Si from NL-hBN/SiO_2/Si structure. Notably, this enhancement effect of DUV Raman signal of Si reduces as the d_{SiO_2} increases for a given N, as depicted in Figure S1 (Supporting Information), where N varies from 0 to 1000 and d_{SiO_2} varies from 0 to 500 nm.

In the NL-hBN/SiO_2/Si structure, besides I_{2-NL}(Si), Raman signal of hBN flake should be also affected by the interference effect of laser and Raman signal in the multilayered structure. We denote I_{2-NL}(hBN) as Raman intensity of hBN flake from NL-hBN/SiO_2/Si structure. Figure 4(a) is the schematic diagrams for light propagation of laser and Raman signals related to I_{bulk}(Si) and I_{2-NL}(hBN). Figures 4(b) and (c) show the Raman spectra of NL-hBN flakes on SiO_2/Si substrate under 266-nm and 532-nm excitations, respectively. With increasing N, I_{2-NL}(hBN) first increases and then decreases, reaching a maximum at 67L under 266-nm excitation while I_{2-NL} (hBN) is not sensitive to N for the studied flakes ($19 \leq N \leq 78$) under 532-nm excitation. The experimental data of N-dependent I_{2-NL}(hBN)/I_{bulk}(Si) can be well fitted by the calculated results by transfer matrix formalism based on the interference effect in the NL-hBN/SiO_2/Si multilayered structure, as depicted in Figure 4(d) by dashed and solid lines, where the Raman scattering efficiency ratio (η) of hBN to Si is a fitting parameter. η is found to be 0.026 and 0.029 for 532-nm and 266-nm excitations, respectively.

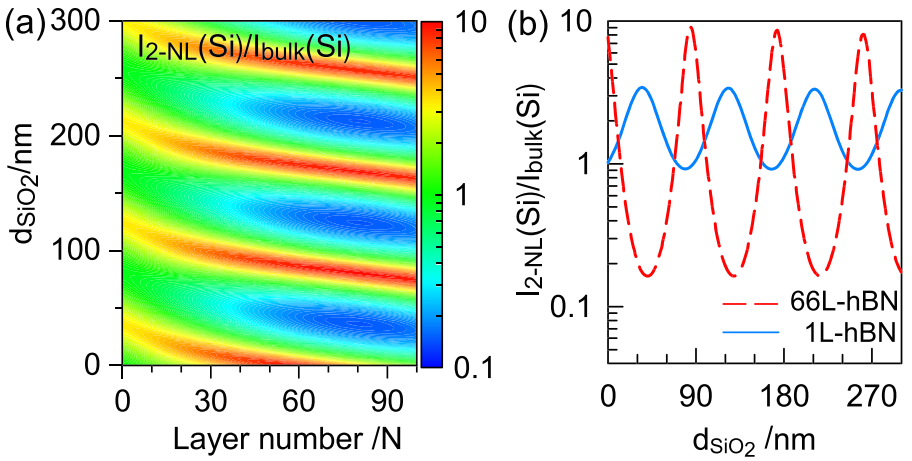

FIGURE 3 (a) The calculated I_{2-NL}(Si)/I_{bulk}(Si) as a function of N and d_{SiO_2}. (b) The calculated I_{2-NL}(Si)/I_{bulk}(Si) as a function of d_{SiO_2}. Dash line, 66L-hBN; solid line, 1L-hBN

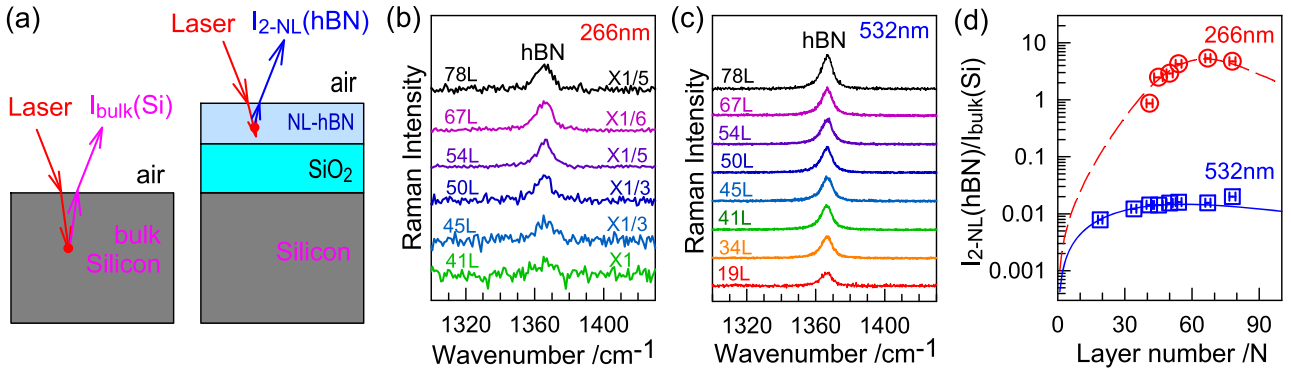

FIGURE 4 (a) Schematic diagrams for light propagation of laser and Raman signals from bulk Si and from hBN flake in the *N*L-hBN/SiO_2/Si structure. Raman spectra of *N*L-hBN flakes on 90-nm SiO_2/Si substrates excited by (b) 266-nm and (c) 532-nm lasers. (d) I_{2-NL}(hBN)/I_{bulk}(Si) as a function of *N* when d_{SiO_2}=90 nm. The dash and solid lines indicate the calculated results while circles and squares are the experimental data

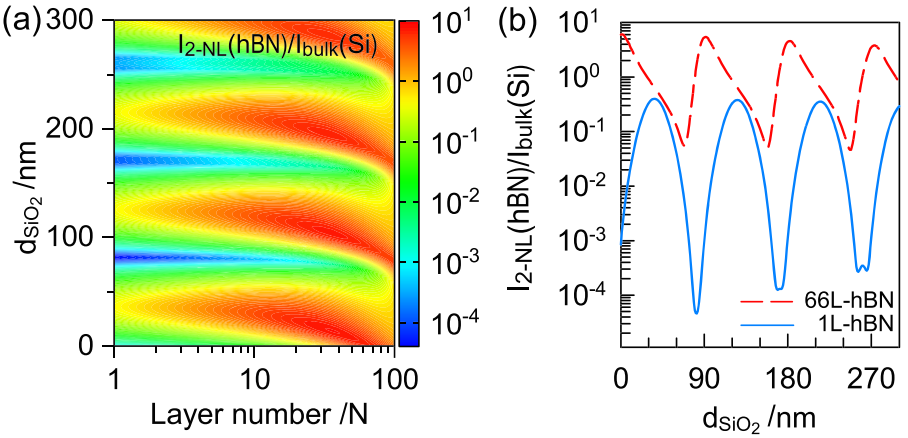

FIGURE 5 (a) The calculated I_{2-NL}(hBN)/I_{bulk}(Si) as a function of *N* and d_{SiO_2}. (b) The calculated I_{2-NL}(hBN)/I_{bulk}(Si) as a function of d_{SiO_2}. Dash line, 66L-hBN; solid line, 1L-hBN

Figure 4(d) demonstrates that I_{2-NL}(hBN) can vary by up to ~4 and 1 orders of magnitude with increasing *N* under 266-nm and 532-nm excitations, respectively. It shows again that the interference effect on the Raman intensity from the *N*L-hBN/SiO_2/Si multilayered structure is significantly different for DUV and visible excitations, similar to the case in Figure 2(e). This is also the reason why the experimental I_{2-NL}(hBN)/I_{bulk}(Si) excited by 266 nm laser is larger than that excited by 532 nm laser by ~3 orders of magnitude. It should be pointed out that as *N* further increases, the I_{2-NL}(hBN)/I_{bulk}(Si) does not decrease monotonously, but shows clearly oscillation under both 266-nm and 532-nm excitations, as depicted in Figure S2 (Supporting Information), where *N* varies from 0 to 1000.

The huge variation of I_{2-NL}(hBN) with *N* indicates constructive or destructive interference in the multilayered structure to the Raman intensity. Thus, an appropriate d_{SiO_2} can be chosen to enhance I_{2-NL}(hBN). We calculated I_{2-NL}(hBN)/I_{bulk}(Si) as a function of *N* and d_{SiO_2} by transfer matrix formalism under 266-nm excitation, as shown in Figure 5(a). For different d_{SiO_2}, I_{2-NL}(hBN) can reach its maximum at different *N*. The case of d_{SiO_2} = 90 nm is shown by the dash line in Figure 4(d). For a fixed *N*, I_{2-NL}(hBN) can vary in a large range with increasing d_{SiO_2}. The curves of I_{2-NL}(hBN)/I_{bulk}(Si) for *N* = 1 and *N* = 66 are given in Figure 5(b). I_{2-NL}(hBN)/I_{bulk}(Si) varies by ~2 orders of magnitude for *N* = 66 and ~4 orders of magnitude for *N* = 1. Therefore, for a given *N*, an appropriate d_{SiO_2} is also a critical factor to enhance DUV Raman signal of I_{2-NL}(hBN) from the *N*L-hBN/SiO_2/Si structure. For example, we can choose d_{SiO_2} = 90 nm and 300 nm to enhance Raman signal of 66L-hBN and 1L-hBN under the 266-nm excitation, respectively. We also calculated I_{2-NL}(hBN)/I_{bulk}(Si) as a function of *N* and d_{SiO_2} in a larger range, and the corresponding result is depicted in Figure S3 in the Supporting Information, from which one can choose appropriate d_{SiO_2} to

access the maxima of I_{2-NL}(Si) and I_{2-NL}(hBN) from the NL-hBN/SiO_2/Si structure for a given N.

4 | CONCLUSION

In conclusion, we took hBN flake deposited on SiO_2/Si substrates as an example to demonstrate how to enhance DUV Raman signal from the hBN flake and its underlying Si substrate. We found that under 266-nm excitation, I_{2-NL}(Si) and I_{2-NL}(hBN) are significantly dependent on d_{SiO_2}, which can be reproduced by the simulation based on the interference effect in the multilayered structure formed by hBN flake and SiO_2/Si substrate. For a fixed N, some specific d_{SiO_2} can be chosen to enhance I_{2-NL}(Si) and I_{2-NL}(hBN) from the hBN/SiO_2/Si structure, and the corresponding Si and hBN Raman intensity can vary by up to $\sim$ 2 and $\sim$4 orders of magnitude, respectively. This work paves the way for the researches of DUV Raman spectroscopy of two-dimensional materials and their substrates.

ACKNOWLEDGEMENT

We acknowledge support from the National Key Research and Development Program of China (Grant No. 2016YFA0301204), the National Natural Science Foundation of China (Grant No. 11874350 and 12004377), CAS Key Research Program of Frontier Sciences (Grant No. ZDBS-LY-SLH004), Project funded by China Postdoctoral Science Foundation (Grant No. 2019TQ0317).

ORCID

Miao-Ling Lin https://orcid.org/0000-0001-5838-8237

REFERENCES

[1] L. Bergman, R. J. Nemanich, *Annu. Rev. Mater. Sci.* **1996**, *26*, 551.
[2] A. Jorio, M. S. Dresselhaus, R. Saito, G. Dresselhaus, *Raman Spectroscopy in Graphene Related Systems*, John Wiley & Sons **2011**.
[3] P. H. Tan, *Raman Spectroscopy of Two-Dimensional Materials*, Springer Nature Singapore Pte Ltd. **2019**.
[4] M. Karim, J. M. J. Lopes, M. Ramsteiner, *J. Raman Spectrosc.* **2020**, *51*, 2468.
[5] X. Zhang, X. F. Qiao, W. Shi, J. B. Wu, D. S. Jiang, P. H. Tan, *Chem. Soc. Rev.* **2015**, *44*, 2757.
[6] X. Cong, M. L. Lin, P. H. Tan, *J. Semicond.* **2019**, *40*, 091001.
[7] G. A. N. Connell, R. J. Nemanich, C. C. Tsai, *Appl. Phys. Lett.* **1980**, *36*, 31.
[8] Y. Y. Wang, Z. H. Ni, Z. X. Shen, H. M. Wang, Y. H. Wu, *Appl. Phys. Lett.* **2008**, *92*, 043121.
[9] D. Yoon, H. Moon, Y. W. Son, J. S. Choi, B. H. Park, Y. H. Cha, Y. D. Kim, H. Cheong, *Phys. Rev. B* **2009**, *80*, 125422.
[10] X. L. Li, X. F. Qiao, W. P. Han, Y. Lu, Q. H. Tan, X. L. Liu, P. H. Tan, *Nanoscale* **2015**, *7*, 8135.
[11] Z. H. Ni, H. M. Wang, J. Kasim, H. M. Fan, T. Yu, Y. H. Wu, Y. P. Feng, Z. X. Shen, *Nano Lett.* **2007**, *7*, 2758.
[12] W. P. Han, Y. M. Shi, X. L. Li, S. Q. Luo, Y. Lu, P. H. Tan, *Acta Phys. Sin.* **2013**, *62*, 110702.
[13] Y. K. Koh, M. H. Bae, D. G. Cahill, E. Pop, *ACS Nano* **2011**, *5*, 269.
[14] X. L. Li, X. F. Qiao, W. P. Han, X. Zhang, Q. H. Tan, T. Chen, P. H. Tan, *Nanotechnology* **2016**, *27*, 145704.
[15] D. E. Aspnes, A. A. Studna, *Phys. Rev. B* **1983**, *27*, 985.
[16] C. Casiraghi, A. Hartschuh, E. Lidorikis, H. Qian, H. Harutyunyan, T. Gokus, K. S. Novoselov, A. C. Ferrari, *Nano Lett.* **2007**, *7*, 2711.
[17] D. M. Hoffman, G. L. Doll, P. C. Eklund, *Phys. Rev. B* **1984**, *30*, 6051.
[18] A. Segura, L. Artús, R. Cuscó, T. Taniguchi, G. Cassabois, B. Gil, *Phys. Rev. Mater.* **2018**, *2*, 024001.

SUPPORTING INFORMATION

Additional supporting information may be found in the online version of the article at the publisher's website.

How to cite this article: T. Liu, M.-L. Lin, Y.-C. Leng, X. Cong, X. Zhang, P.-H. Tan, *J Raman Spectrosc* **2021**, *52*(12), 2160. https://doi.org/10.1002/jrs.6228